



Simulation of GISAXS Experiments with BornAgain

Julia Schäfer, University of Tübingen, Germany

September 10, 2015

Supervisor: Peng Zhang

Abstract

In this report my work during the DESY Summer Student Programme 2015 in the group FS-PE is presented. My task was to do simulations of GISAXS experiments by using the relatively new software package BornAgain ¹. The considered experiment was the airbrush-spray deposition of gold nanoparticles and a diblock copolymer on a Si substrate.

¹C. Durniak, M. Ganeva, G. Pospelov, W. Van Herck, J. Wuttke (2015), BornAgain — Software for simulating and fitting X-ray and neutron small-angle scattering at grazing incidence, version 1.3.0, <http://www.bornagainproject.org>

Contents

1	Introduction	3
2	Theory	3
2.1	GISAXS	3
2.2	BornAgain	7
3	Experimental	8
4	Results	10
4.1	Experimental Results	10
4.2	Simulation of the Dried State	14
4.3	Simulation of the Drying Process	16
5	Conclusion	22

1 Introduction

Polymer nanocomposites consist of a polymer matrix to which nanoparticles were added. These systems are promising for the achievement of nanoscopic organization of nanoparticles. This ordering of the particles would be highly desirable in order to fully exploit their potential. For instance, after having formed arrays of gold nanoparticles with 3D ordering, nanocomposites show an optical anisotropy that is wavelength-dependent. [1]

One relatively novel method of coating substrates with nanocomposites is airbrush-spray deposition. The advantages of this technique are that it is fast and uncomplicated. Moreover, it is low-cost and can be reproduced. [2]

Here the self-assembly of a sample is investigated that was airbrush spray-deposited onto a Si substrate. The deposited system consisted of a diblock copolymer and gold nanoparticles that were suspended in an equal volume mixture of water and ethanol.

The experimental method used to analyze the ordering was Grating Incidence Small Angle X-Ray Scattering (GISAXS) as it is perfectly suited to investigate nanostructured polymer films. The underlying reason is that not only the surface is probed, but also the buried structure. [3]

In order to fully understand the obtained GISAXS patterns, it is necessary to conduct simulations. In this project the new software package BornAgain was used (see section 2.2) to mimic the experimental GISAXS pattern of the dried state. Apart from that the drying process was simulated to achieve a deeper understanding of the nanoparticles' self-assembly.

2 Theory

2.1 GISAXS

The abbreviation GISAXS stands for Grating Incidence Small Angle X-Ray Scattering. It is a technique to study nanostructured surfaces and thin films. This method was first introduced in 1989 by Levine and Cohen [4].

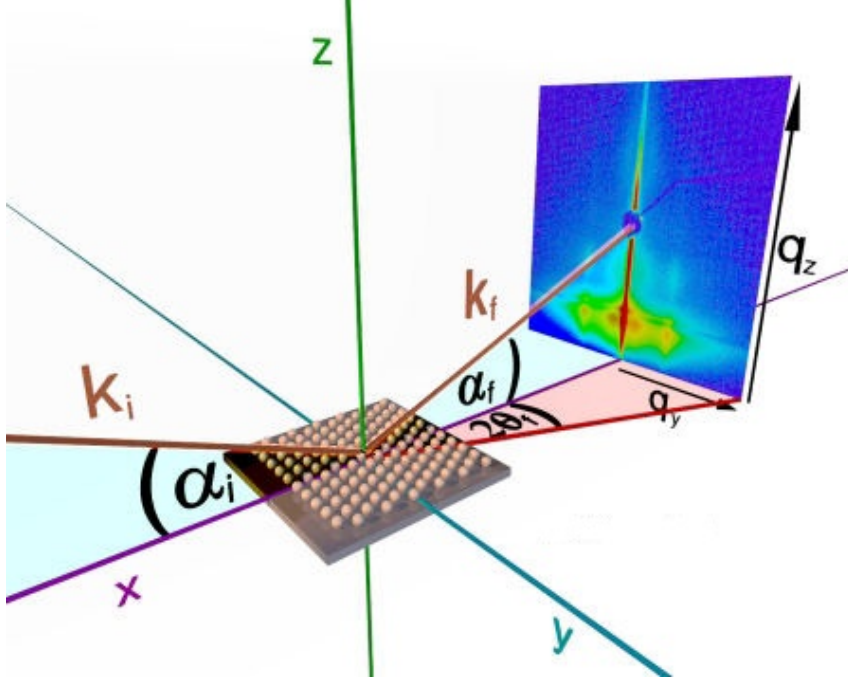


Figure 1: Geometry of a GISAXS experiment [5]

The geometry of a GISAXS experiment is depicted in figure 1. Grazing incidence means that the X-ray beam with the wavevector \vec{k}_i impinges on the sample under a very small incident angle α_i , below 1° in the case of hard X-rays [6]. The scattering is caused by electron density fluctuations in the sample illuminated by the beam and it occurs along \vec{k}_f in the direction $(2\theta_f, \alpha_f)$. The scattering wavevector \vec{q} is defined as

$$\vec{q} = \vec{k}_i - \vec{k}_f \quad (1)$$

and can be calculated with the following equation

$$\vec{q} = \frac{2\pi}{\lambda} \begin{pmatrix} \cos(\alpha_f)\cos(2\theta_f) - \cos(\alpha_i) \\ \cos(\alpha_f)\sin(2\theta_f) \\ \sin(\alpha_f) + \sin(\alpha_i) \end{pmatrix} \quad (2)$$

The scattering intensity $I(\vec{q})$ can be expressed as [5]

$$I(\vec{q}) = \langle |F|^2 \rangle S(q_{\parallel}) \quad (3)$$

where F is the form factor and $S(q)$ is the total interference function. The interference function indicates how the objects are arranged on the surface. In the Born Approximation (BA) the form factor F is the Fourier transform of the electron density distribution of the objects. However, the BA is not sufficient if multiple reflections and refractions at interfaces have to be taken into account. In that case,

the distorted wave Born approximation (DWBA) has to be used. It is a first order correction to the scattering theory.

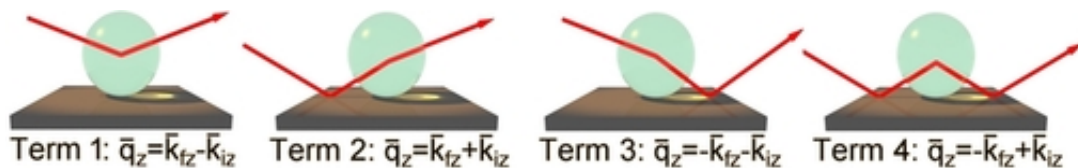


Figure 2: DWBA [5]

In figure 2 the four terms of the DWBA are illustrated. The first thereof is known from the Born Approximation. These four expressions are associated to different scattering events, involving or not a reflection of either the incident beam or the final beam. Each term is weighted with the corresponding Fresnel coefficients. The waves created in this manner interfere coherently and lead to the effective form factor.

An advantage of GISAXS over scanning probe microscopy methods such as AFM and STM is that not only the surface structure is examined but also buried structures in thin films. The scattering depth Λ can be adjusted by varying the incident angle α_i according to the following formula

$$\Lambda = \frac{\lambda}{\sqrt{2\pi}} \cdot \frac{1}{\sqrt{\sqrt{(\alpha_i^2 - \alpha_c^2)^2 + 4\beta^2} - (\alpha_i^2 - \alpha_c^2)}} \quad (4)$$

α_c is the critical angle of total external reflection and λ is the wavelength of the incident beam. Typically an incident angle α_i slightly above the critical angle α_c is chosen.

The β in equation 4 is the imaginary part of the refractive index n for X-rays

$$n = 1 - \delta + i\beta \quad (5)$$

It depends on the wavelength λ and the absorption coefficient μ as follows

$$\beta = \frac{\lambda}{4\pi} \mu \quad (6)$$

The real part δ can be calculated by

$$\delta = \frac{\lambda^2}{2\pi} r_0 N Z \quad (7)$$

where λ is again the wavelength, r_0 is the classical electron radius (also known as Thomson scattering length), N is the number density of atoms and Z is the atomic number.

Due to equation 5 the refractive index of X-rays in matter is smaller than one which means that the matter is optically less dense for this kind of radiation than vacuum. This results in the fact that the phase velocity of X-rays in matter is higher than the speed of light.

The critical angle of total external reflection α_c is dependent on the investigated material and on the wavelength of the x-rays

$$\alpha_c = \sqrt{2\delta} = \sqrt{2 \frac{\lambda^2}{2\pi} r_0 N Z} \quad (8)$$

Due to the gracing incidence geometry with the small incident angle a large surface area is investigated and thus, a statistical description of the sample over macroscopic length scales is obtained [7]. This makes it advantageous over TEM where only a small area is probed in one measurement and where therefore the acquisition of many images is necessary in order to obtain reliable statistics.

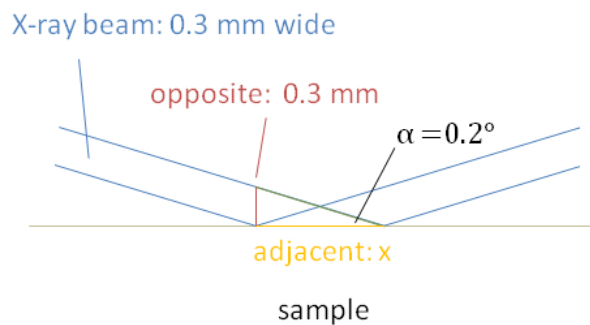


Figure 3: Illustration of the footprint effect

In the following a sample calculation is presented to illustrate this footprint effect. Figure 3 shows the numerical values that were taken from [8]: The considered X-ray beam is 0.3 mm wide. This corresponds to an opposite in the right-angled triangle that has a length of 0.300001828 mm \approx 0.3 mm because of the small entrance angle of $\alpha=0.2^\circ$ of the incoming beam. The adjacent is the sought quantity x that is equivalent to the surface area being hit by the beam. It can be calculated by

$$\tan \alpha = \frac{\text{opposite}}{\text{adjacent}} = \frac{\text{opposite}}{x} \quad (9)$$

$$x = \frac{\text{opposite}}{\tan \alpha} = \frac{0.3 \text{ mm}}{\tan(0.2^\circ)} \approx 86 \text{ mm} = 8.6 \text{ cm} \quad (10)$$

This means that a 0.3 mm wide beam at a typical entrance angle of 0.2° has a large footprint on the sample of 8.6 cm.

GISAXS measurements can be performed both at laboratory sources and at synchrotron radiation sources. However, the full potential of GISAXS can only be exploited at synchrotron facilities due to the high flux and collimation of the radiation created there. Moreover, the wavelength can be adjusted in order to avoid fluorescence or to perform anomalous measurements. [9]

At the so-called Yoneda peak the scattering of the material has its maximum. This feature was discovered in 1963 [10] and occurs if

$$\alpha_{i,f} = \alpha_c \quad (11)$$

The Yoneda peak position is specific for every material and it depends on the electron density: The higher the electron density is, the higher (in q_z direction) is the Yoneda peak.

2.2 BornAgain

BornAgain is an open-source software package for the simulation and the fitting of grazing incidence small angle scattering (GISAS) ². It is free-to-use and can be applied for experiments with both neutrons (GISANS) and with X-rays (GISAXS).

The name BornAgain emphasizes the central role of the distorted-wave Born approximation (DWBA). This is given expression in the fact that the DWBA is automatically applied. Only if particles are embedded in air and not placed on or inside a substrate, the simple Born approximation (BA) is used.

The software package is a further development of IsGISAXS by Rémi Lazzari [11]. The progression is that with BornAgain, among other things, it is possible to define not only one layer and one particle material but an unrestricted number of layers and particle materials.

BornAgain is still further developed by the Scientific Computing Group of the Jülich Centre for Neutron Science (JCNS) at Heinz Maier-Leibnitz Zentrum (MLZ) Garching, Germany. About every two months new major versions are released. The documentation in form of the user manual is incomplete. Therefore users are encouraged to address their questions to the people behind BornAgain, e. g. by using the forum installed on the webpage www.bornagainproject.org.

BornAgain can be applied by either using the Python script or the Graphical User Interface (GUI). However, some things that can be done by using the Python script

²C. Durniak, M. Ganeva, G. Pospelov, W. Van Herck, J. Wuttke (2015), BornAgain — Software for simulating and fitting X-ray and neutron small-angle scattering at grazing incidence, version 1.3.0, <http://www.bornagainproject.org>

have not been implemented into the GUI yet, such as the fitting of experimental GISAXS data.

3 Experimental

A suspension of 20 nm gold nanoparticles and the diblock copolymer PEO(26400)-b-P2VP(5900) in an equal volume solvent mixture of ethanol and water was deposited on a Si wafer substrate by airbrush-spray coating. One spraying period lasted 0.1 s, followed by a drying phase of 10 s. This sequence was repeated ten times and afterwards, the ex situ images were taken.

During spray deposition the sample was heated to 80 °C. The capping agent of the gold particles was PVP with a molecular weight of $8000 \frac{\text{g}}{\text{mol}}$. This ligand layer had a thickness of 1-2 nm according to the producer. The figures 4-6 show the structural formulae of the involved polymers.

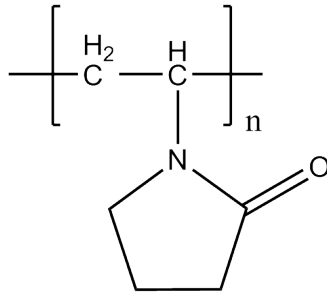


Figure 4: Polyvinylpyrrolidone (PVP)

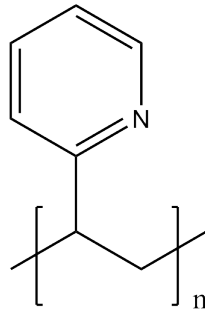


Figure 5: Poly(2-vinylpyridine) (P2VP)

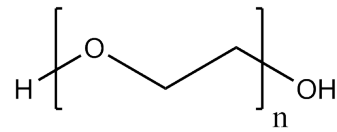


Figure 6: Poly(ethylene oxide) (PEO)

In Figure 7 the GISAXS setup is depicted that was used to monitor ex situ the dried state after the airbrush-spray deposition. Between two measurements the sample was moved in the xy direction to prevent beam damage of the sample. The X-ray beam had a wavelength of 0.095 nm and an inclination angle of 0.45 ° was chosen. The sample detector distance had a value of 3910 ± 4 mm and the air pressure in the airbrush was 1 bar above the ambient pressure. Two beamstops for the direct and the specular beam were used to prevent damage or saturation of the PILATUS 1M detector.

The orange cylinder in figure 7 is made of kapton due to the high transmissivity for X-rays of this material. Through the green tube an argon flow was installed

in order to protect the sample from beam damage. Since the argon atoms absorb the X-rays to a certain extent, they attenuate the beam.

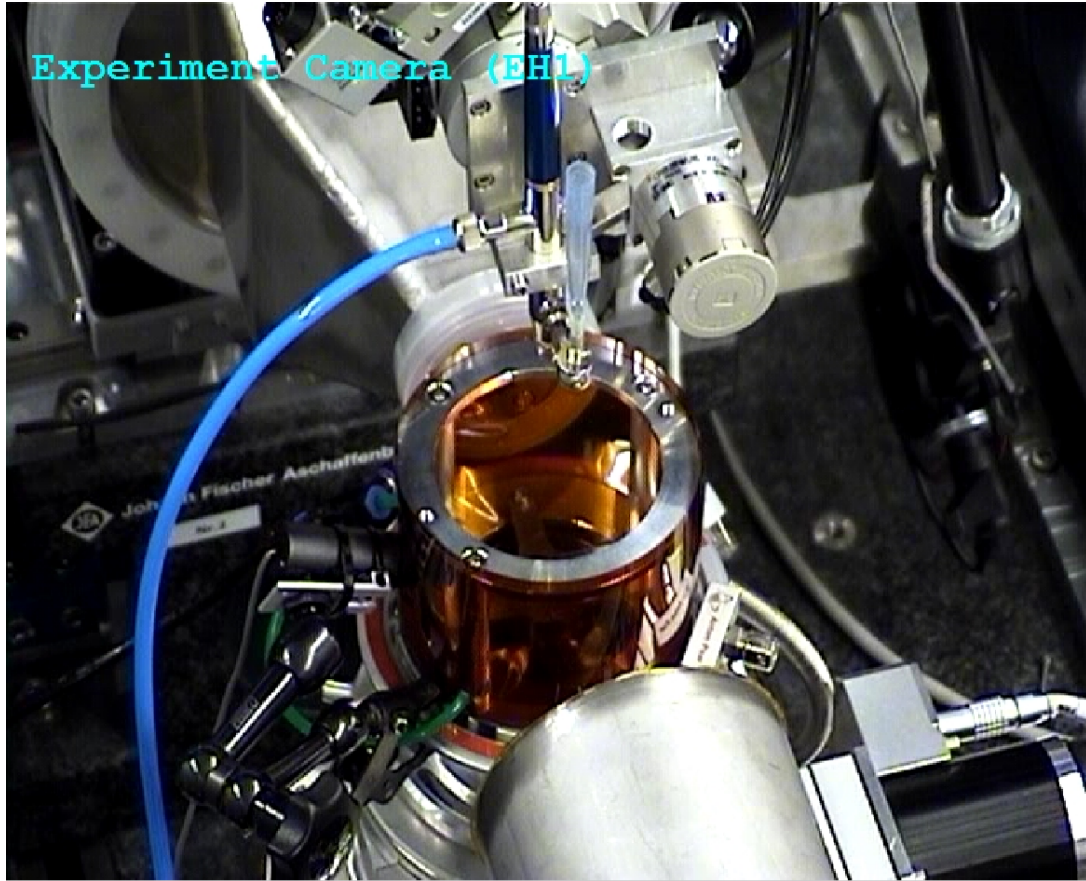


Figure 7: Experimental setup for the in situ GISAXS measurements, including the airbrush (blue) and the kapton cylinder (orange)

The GISAXS measurements were performed at the HASYLAB beamline P03 at the Petra III storage ring. The experimental setup was similar to the one shown in figure 8. The circular area on the Si substrate where droplets were deposited had a diameter of approx. 3 cm. The size of the individual droplets varied between tens and hundreds of microns, according to the droplet size classification system ASABE S-572.1 by the American Society of Agricultural and Biological Engineers. This size range was confirmed by optical microscopy.

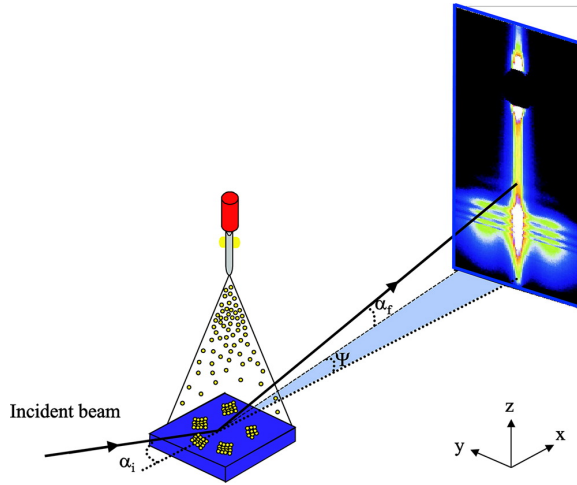


Figure 8: Setup for airbrush-spray deposition experiments [12]

4 Results

4.1 Experimental Results

Apart from the sample with both diblock copolymer molecules and gold nanoparticles, there was also the airbrush-spray deposition of a diblock copolymer sample investigated that did not contain any gold particles. On most of the ex situ images of this system no hints for a lateral ordering could be found, as it is displayed in Figure 9.

On the contrary, there is a blurred signal resulting from lateral ordering in the ex situ images of the sample containing both gold nanoparticles and the diblock copolymer (see Figure 10). The smudginess means that there is some organisation in the xy-plane. However, it is not regular. Since otherwise, one would observe sharp maxima in the horizontal GISAXS pattern. From the figures 9 and 10 one can therefore draw the conclusion that the addition of gold particles promotes ordering in the spray-deposited system.

An average distance of 30 nm between the gold nanoparticles was calculated from the experimental GISAXS data by analyzing horizontal cuts that were obtained with DPDAK, an open source tool developed for the analysis of large sequences of small angle scattering data [13]. In figure 11 an experimental GISAXS pattern and the correspondig horizontal cut are displayed. It was found that the average position of the first maximum was 0.20944 nm^{-1} . From this, the mean distance between two particles d was calculated with the known conversion from reciprocal into real space

$$d = \frac{2\pi}{0.20944 \text{ nm}^{-1}} \approx 30.0 \text{ nm} \quad (12)$$

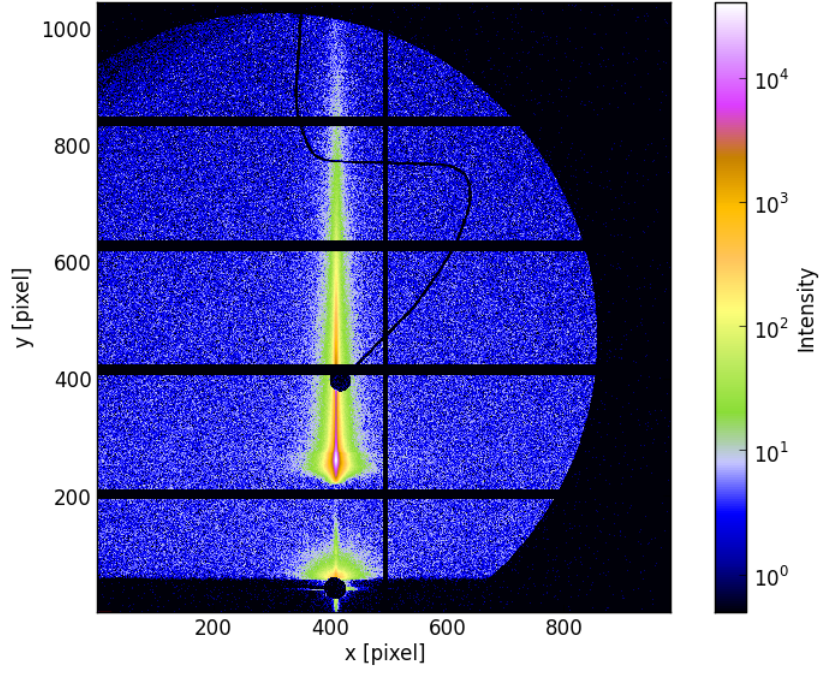


Figure 9: Ex situ GISAXS image of the diblock copolymer sample without gold particles

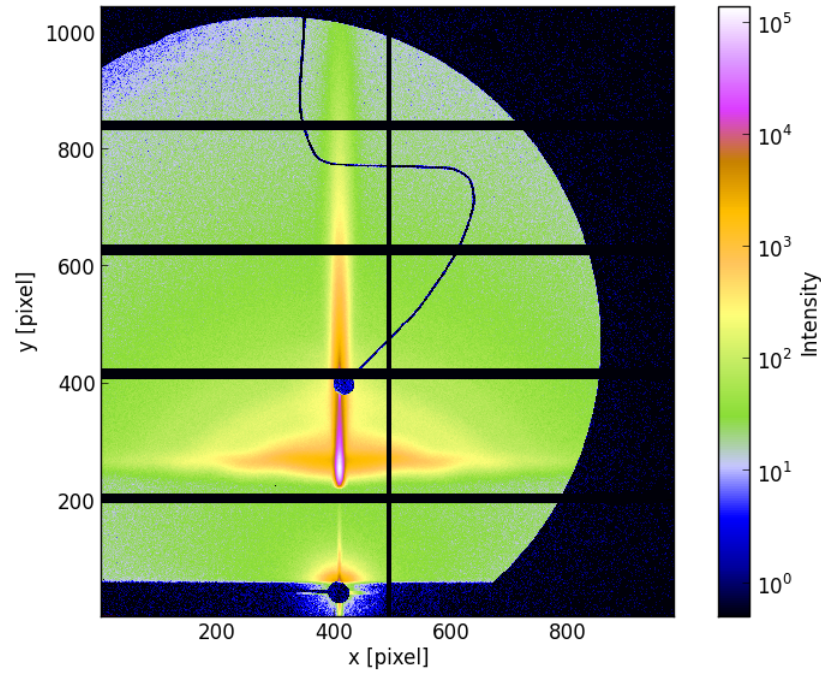


Figure 10: Ex situ GISAXS image of the diblock copolymer mixed with 20 nm gold nanoparticles

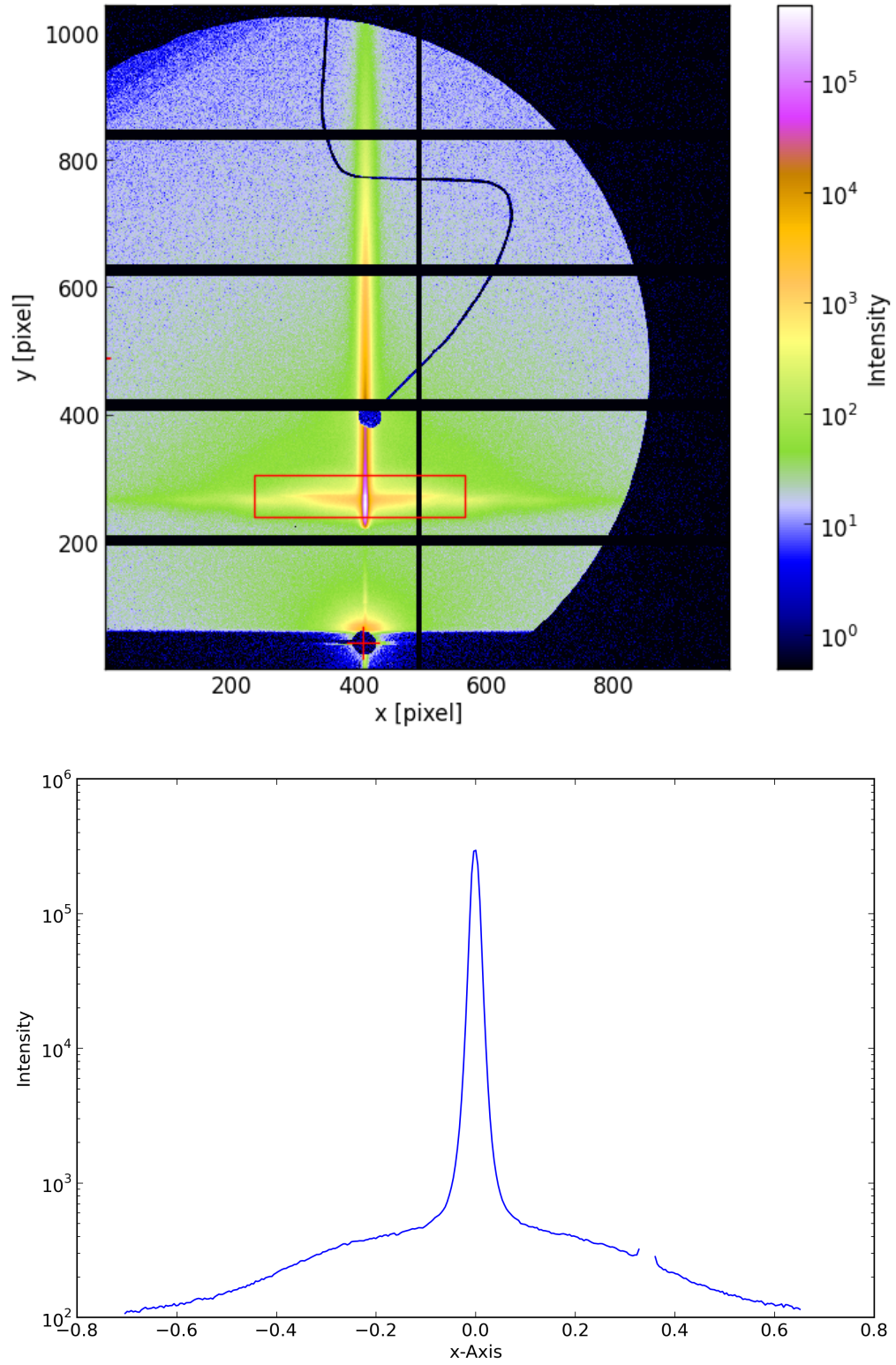


Figure 11: The experimental ex situ GISAXS pattern (top) with the area within the red box that was used for the horizontal cut (bottom)

The AFM image in figure 12 depicts the spray-deposited sample that was heated to 80°C and contained both the diblock copolymer and the gold nanoparticles. It was taken in ambient air and with intermittent contact of a cantilever with a force constant of $22\text{-}100 \frac{\text{N}}{\text{m}}$. The AFM was purchased from NT-MDT. What one can see in the pictures is that the roughness is very low and from that one can conclude that a polymer layer structure is formed.

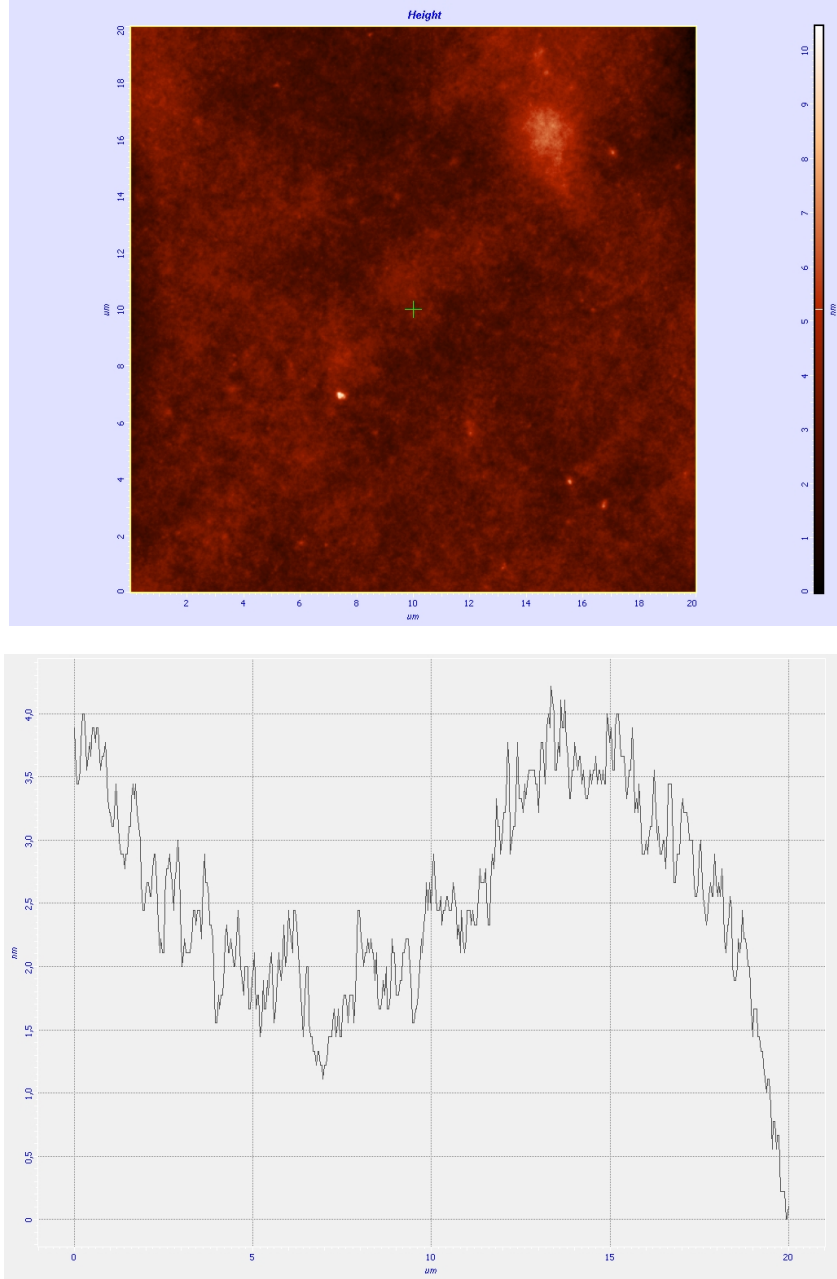


Figure 12: AFM image (top) and corresponding height profile (bottom)

4.2 Simulation of the Dried State

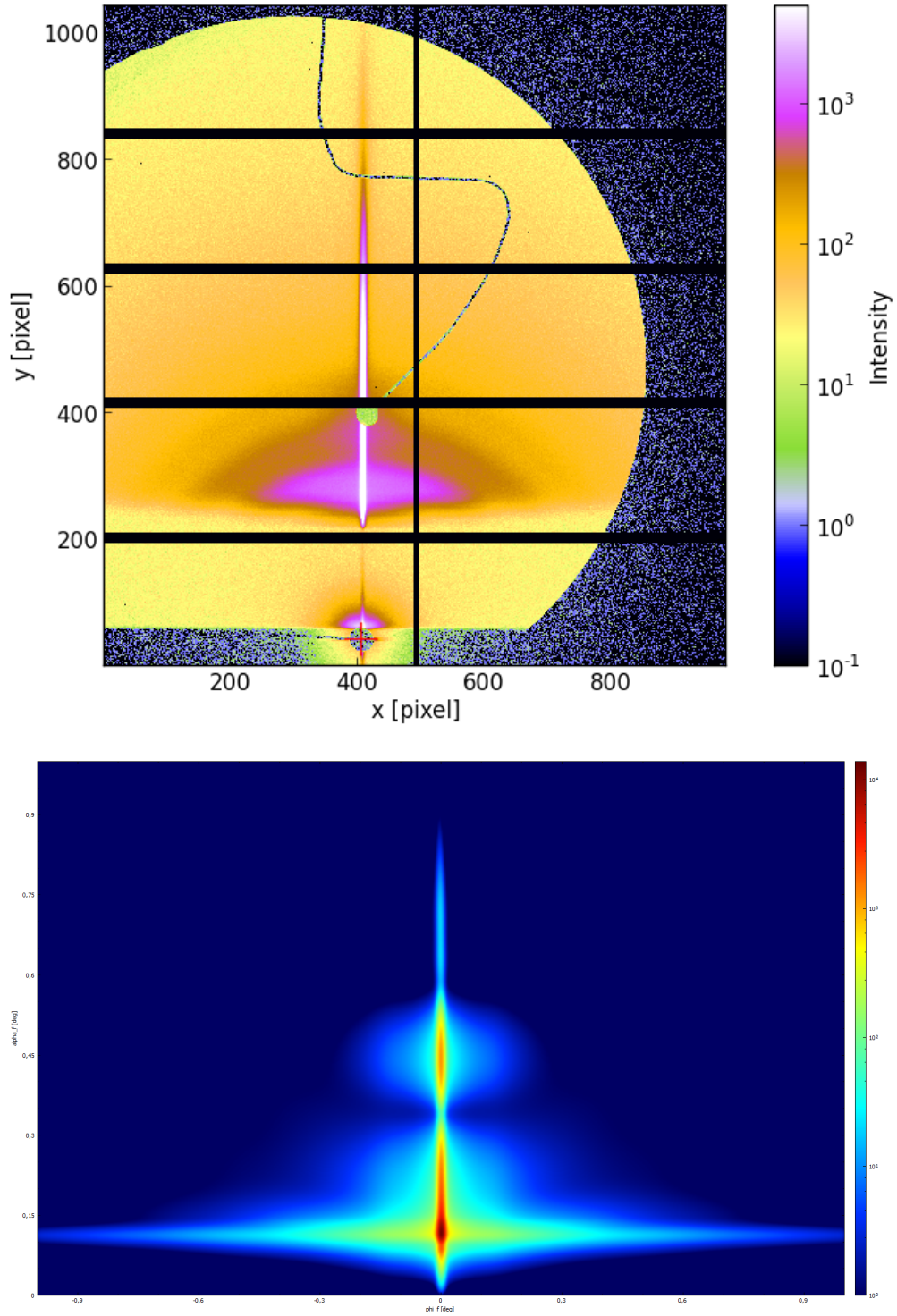


Figure 13: Experimental (top) and simulated GISAXS image (bottom)

The sketch in figure 14 shows the arrangement that was assumed in order to obtain the simulated GISAXS pattern in figure 13 by using the software BornAgain.

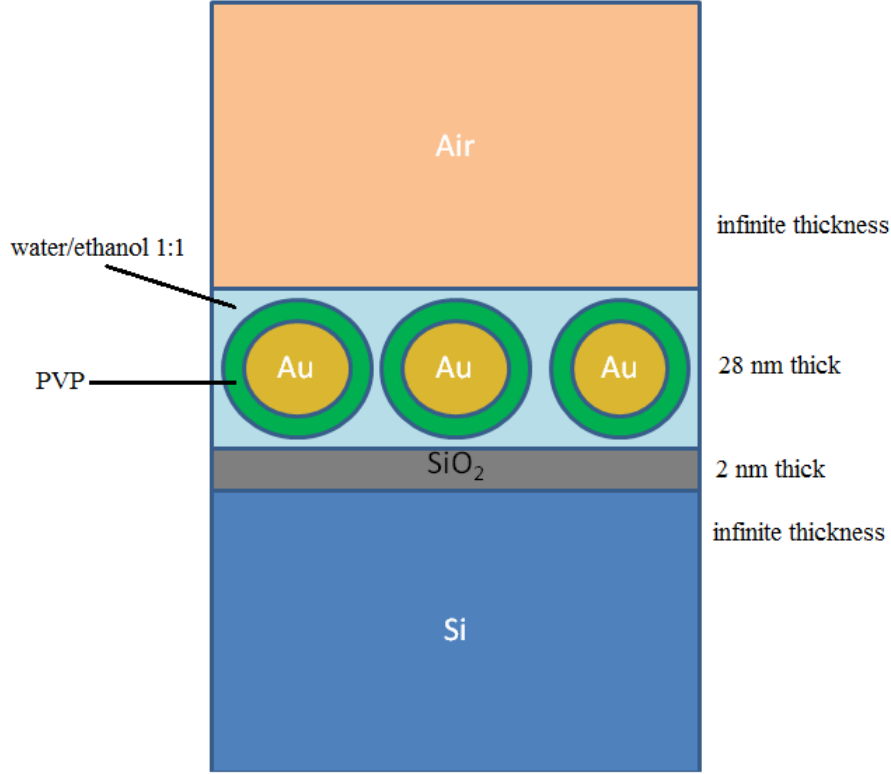


Figure 14: Sketch to illustrate the simulation of the dried state

The bottom Si and the top air layer had an infinite thickness in the simulation. All materials were defined by their complex refractive index for X-rays with a wavelength of 0.095 nm as in the experiment. The values for the refractive index were taken from the Henke tables [14]. The thickness of the SiO₂ layer was chosen to be 2 nm as a thickness of 2.02 ± 0.02 nm was measured by ellipsometry with a laser wave length of 532 nm. Above the silicon substrate the layer with the equal volume solvent mixture of ethanol and water was placed with a thickness of 28 nm. In this layer the gold nanoparticles were embedded. They were defined as core shell particles: They had a gold core with a radius of 10 nm and a PVP shell with an additional thickness of 2 nm³. The particles were arranged in a hexagonal 2D paracrystal with a lattice length of 30 nm due to the experimental data (see section 4.1). The chosen damping length was 5000 nm. The domain size was 1000 nm in both directions. There was no integration over xi turned on and no rotation angle was used. As probability distribution functions (PDF) two Gaussian 2D functions were used: The first one with a gamma value of 10.00 and correlation lengths in

³According to the producer of the gold nanoparticles *Nanopartz*, the PVP ligand layer has a thickness of 1-2 nm.

x- and y-direction of 7.00 nm. The second PDF had a gamma value of 10.00 and correlation lengths in x- and y-direction of 15.00 nm.

Unlike in the simulations in section 15 a distribution of the particle size was introduced to reproduce the experimental image best. This was done by defining a Gaussian distribution with a mean value of 10 nm, a standard deviation of 2, a number of samples of 100 and a sigma factor of 4.71. This means that there was some deviation in the size of the gold core, but not in the PVP shell of the nanoparticles.

Comparing the experimental and simulated GISAXS pattern in figure 13, one finds a satisfactory agreement between simulation and experiment. However, improvements can certainly be done, e. g. more layers of nanoparticles should be included. Furthermore, efforts should be made to obtain AFM or TEM images with higher resolution to find out more about the spatial arrangement of the gold particles and the diblock copolymer on the substrate. With this information a further development of the simulations would be easier.

4.3 Simulation of the Drying Process

The software package BornAgain was used to simulate in situ GISAXS images of the drying process after spray-deposition of the suspension on the Si substrate. To this end, an arrangement of the different materials was assumed as it is illustrated in figure 15.

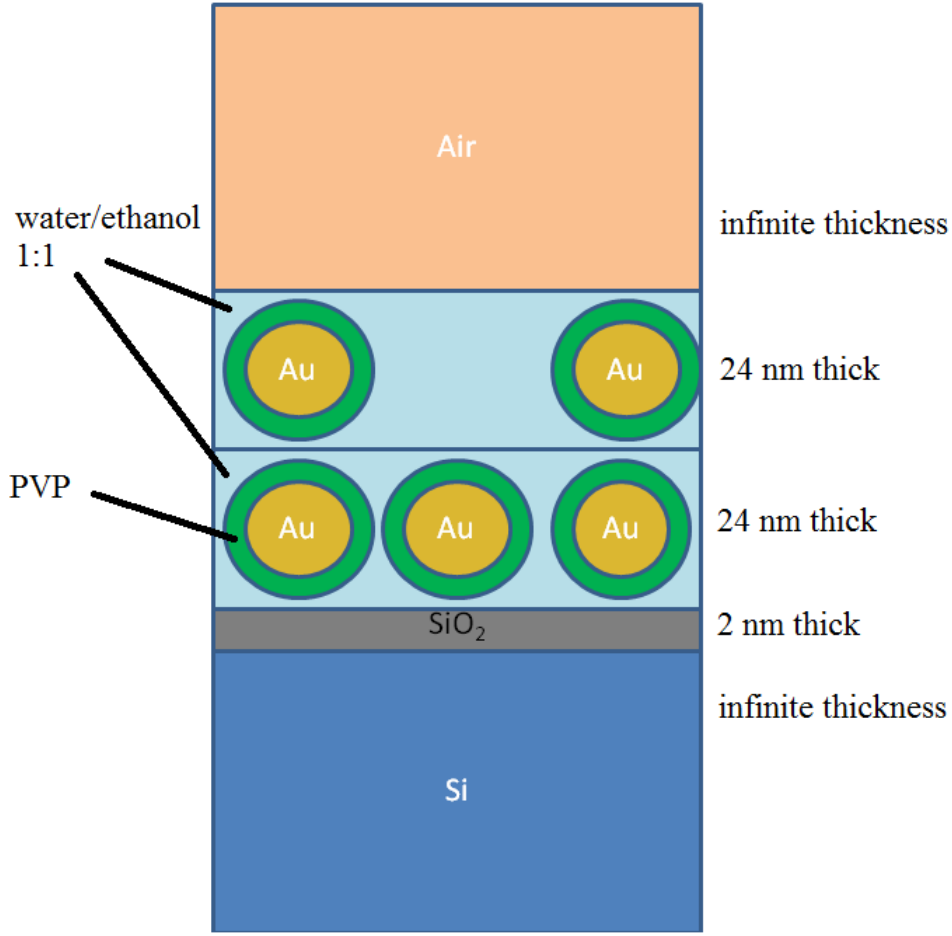


Figure 15: Sketch to illustrate the simulation of the drying process

The bottom Si and the top air layer had an infinite thickness in the simulation. All materials were defined by their complex refractive index for X-rays with a wavelength of 0.095 nm as in the experiment. The values for the refractive index were taken from the Henke tables [14]. The thickness of the SiO_2 layer was chosen to be 2 nm as a thickness of 2.02 ± 0.02 nm was measured by ellipsometry with a laser wavelength of 532 nm. Above the silicon substrate the layer with the equal volume solvent mixture of ethanol and water was placed with a thickness of 24 nm. In this layer the gold nanoparticles were embedded. They were defined as core shell particles: They had a gold core with a radius of 10 nm and a PVP shell with an additional thickness of 2 nm ⁴. In order to mimic the drying process, the distance between two gold particles was gradually decreased from 500 to 100 and 50 and

⁴According to the producer of the gold nanoparticles *Nanopartz*, the PVP ligand layer has a thickness of 1-2 nm.

down to 30 nm. The final distance 30 nm was chosen due to the experimental data (see section 4.1). The diblock copolymer was not included because it was clear from the simulated patterns that the scattering was caused by the gold particles for the predominant part. The presence or absence of an additional copolymer layer had hardly any influence on the simulated GISAXS image.

In more detail, the particles were arranged in the equal volume mixture of water and ethanol in a hexagonal 2D paracrystal with a lattice length of 500, 100, 50 and 30 nm, respectively. The chosen damping length was 5000 nm. The domain size was 1000 nm in both directions. There was no integration over ξ turned on and no rotation angle was used. As probability distribution functions (PDF) two Gaussian 2D functions were used: The first one with a gamma value of 10.00 and correlation lengths in x- and y-direction of 7.00 nm. The second PDF had a gamma value of 10.00 and correlation lengths in x- and y-direction of 15.00 nm.

The result of this simulation sequence is shown in figure 16. On all the following simulations of the drying process the same scale bar was used (1-20000) to allow for better comparison.

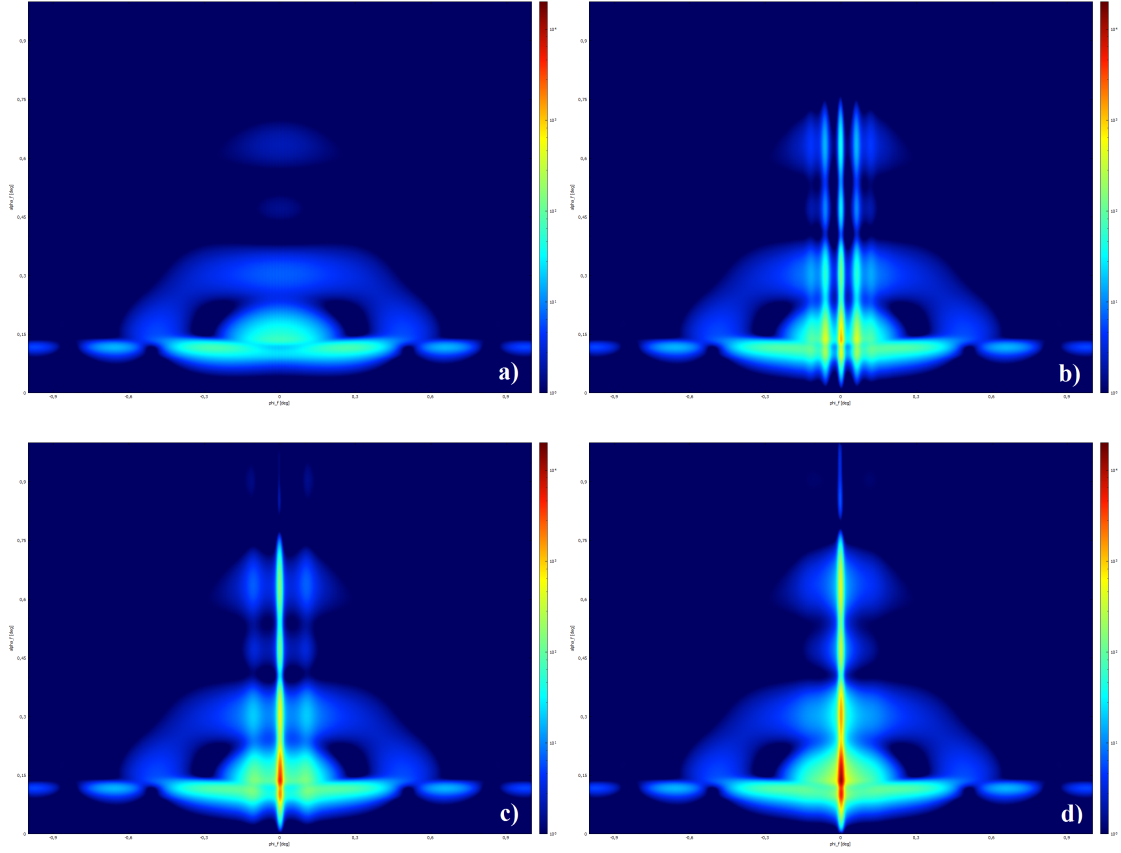


Figure 16: Simulation of the drying process with one layer of gold particles, lattice length decreasing from 500 (a) to 100 (b) and 50 (c) and down to 30 nm (d)

In a second step, the same procedure was conducted for a second layer that was placed on top of the layer with a lattice length of 30 nm. This means that the lattice length of the 2D paracrystal of gold particles in the second layer was decreased from 500 to 100 and 50 and down to 30 nm. All parameters such as the damping length, etc. had the same value as in the case of only one layer of gold particles. Figure 17 illustrates the arrangement of the layers, particles and materials and figure 18 displays the simulated GISAXS patterns.

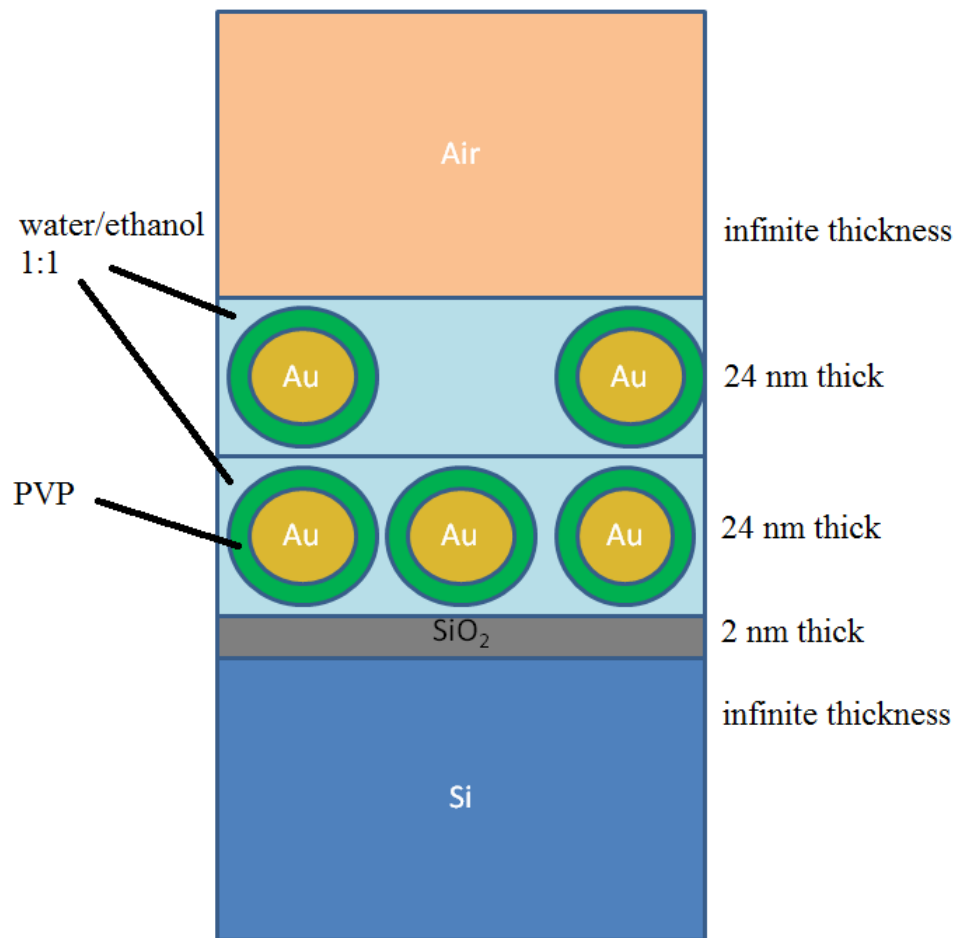


Figure 17: Sketch for the simulation of the drying process with multiple layers

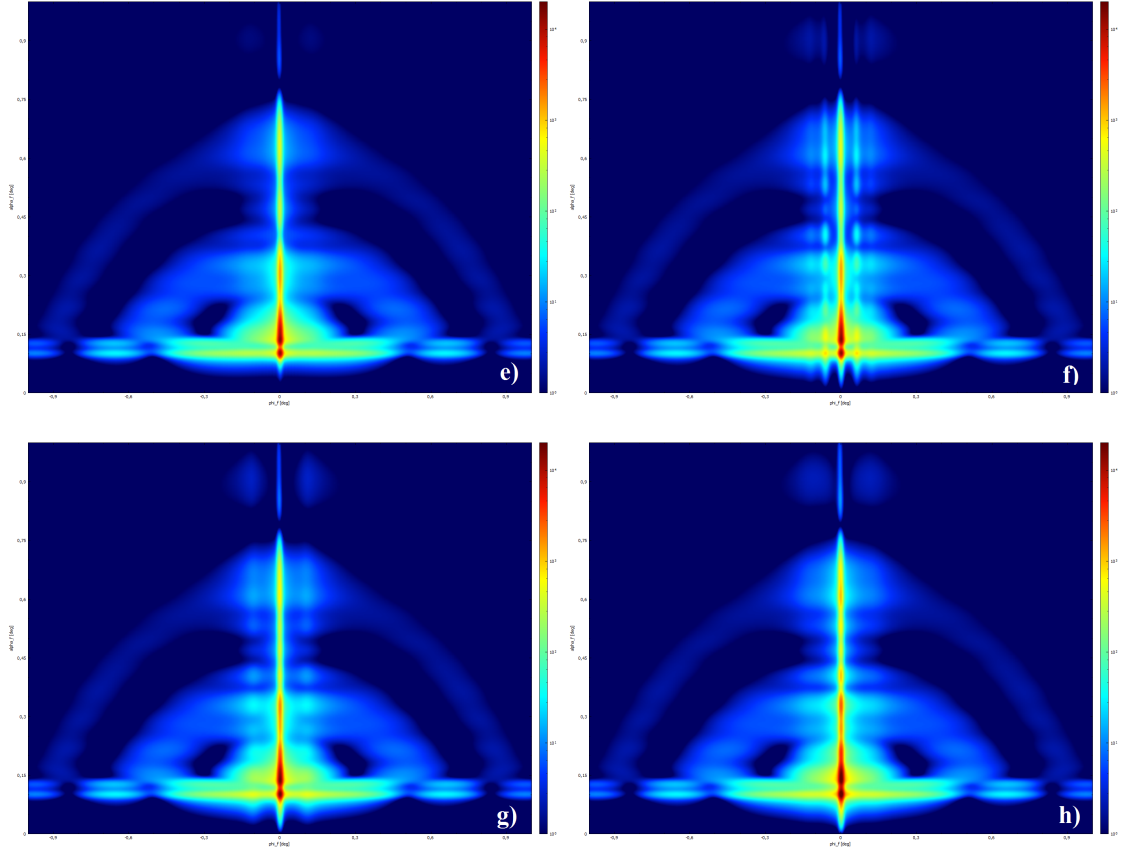


Figure 18: Simulation of the drying process with two layers of gold particles, lattice length of the paracrystalline arrangement of the gold particles in the second layer decreasing from 500 (e) to 100 (f) and 50 (g) and down to 30 nm (h)

A third layer was included in an analogous way: The layer with the decreasing lattice length was put on top of two layers with a lattice length of 30 nm. The resulting GISAXS images are shown in figure 19.

What can be learned from these simulations of the drying process is that the higher order „haloes“ become more intense, the higher the number of layers is. This is due to the fact that the periodicity in z-direction increases with the number of gold particle layers. The comparison of these simulations with experimental data will facilitate the comprehension of future experiments.

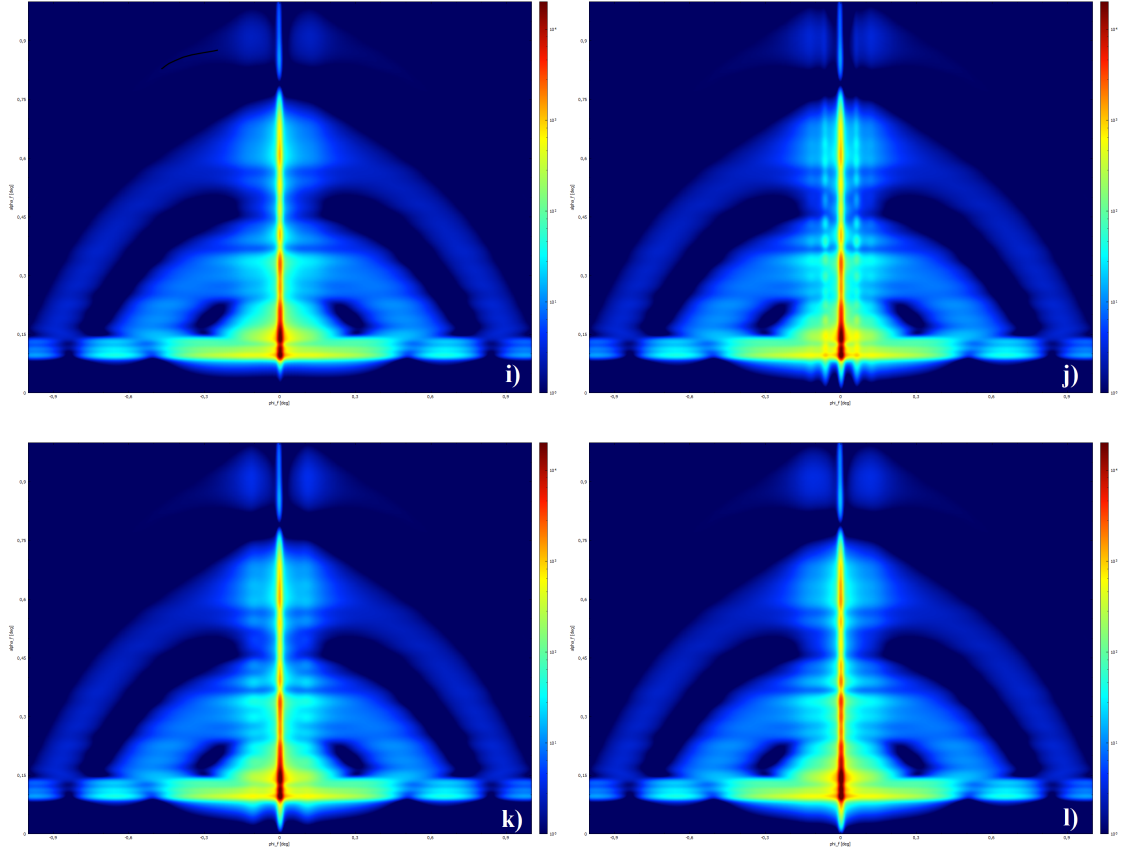


Figure 19: Simulation of the drying process with three layers of gold particles, lattice length of the paracrystalline arrangement of the gold particles in the third layer decreasing from 500 (i) to 100 (j) and 50 (k) and down to 30 nm (l)

5 Conclusion

In this work the self-assembly of nanocomposites following airbrush-spray deposition was investigated. It was found out that the additional presence of gold nanoparticles in the suspension, beside the diblock copolymer, promotes ordering during the drying process. Furthermore, it could be shown that the new software BornAgain is well-suited for the simulation of GISAXS pattern resulting from complex nanostructures.

References

- [1] Kao, J.; Thorkelsson, K.; Bai, P.; Zhang, Z.; Sun, C. and Xu, T., *Nat. Commun.*, 2014, **5**, 1 – 8.
- [2] Herzog, G.; Benecke, G.; Buffet, A.; Heidmann, B.; Perlich, J.; Risch, J.; Santoro, G.; Schwartzkopf, M.; Yu, S.; Wurth, W. and Roth, S., *Langmuir*, 2013, **29**, 11260 – 11266.
- [3] Müller-Buschbaum, P., *Anal. Bioanal. Chem.*, 2003, **376**, 3 – 10.
- [4] Levine, J.; Cohen, J.; Chung, Y. and Georgopoulos, P., *J. Appl. Cryst.*, 1989, **22**, 528 – 532.
- [5] <http://www.gisaxs.de/theory.html> (09/05/2015).
- [6] Hexemer, A. and Müller-Buschbaum, P., *IUCrJ*, 2015, **2**, 106 – 125.
- [7] Jiang, Z.; Lee, D.; Narayanan, S.; Wang, J. and Sinha, S., *Phys. Rev. B.*, 2011, **84**, 075440.
- [8] Schnablegger, H. and Singh, Y., *The SAXS Guide*, Anton Paar GmbH, 3 ed., 2013.
- [9] Ezquerro, T.; García-Gutiérrez, M.; Nogales, A. and Gómez, M., Eds., *Applications of Synchrotron Light to Scattering and Diffraction in Materials and Life Sciences*, Springer-Verlag Berlin Heidelberg, 2009.
- [10] Yoneda, Y., *Phys. Rev.*, 1963, **131**(5), 2010 – 2013.
- [11] Lazzari, R., *J. Appl. Cryst.*, 2002, **35**, 406 – 421.
- [12] Al-Hussein, M.; Schindler, M.; Ruderer, M.; Perlich, J.; Schwartzkopf, M.; Herzog, G.; Heidmann, B.; Buffet, A.; Roth, S. and Müller-Buschbaum, P., *Langmuir*, 2013, **29**, 2490 – 2497.
- [13] Benecke, G.; Wagermaier, W.; Li, C.; Schwartzkopf, M.; Flucke, G.; Hoerth, R.; Zizak, I.; Burghammer, M.; Metwalli, E.; Müller-Buschbaum, P.; Trebbin, M.; Förster, S.; Paris, O.; Roth, S. and Fratzl, P., *J. Appl. Cryst.*, 2014, **47**, 1797 – 1803.
- [14] Henke, B.; Gullikson, E. and Davis, J., *X-ray interactions: photoabsorption, scattering, transmission, and reflection at E=50-30000 eV, Z=1-92*, Vol. 54, Atomic Data and Nuclear Data Tables, 1993.